Thermo X https://doi.org/10.70401/tx.2026.0029

Supplementary information

Combined normal and inverse barocaloric effect materials

Lingli Li, Haoyu Wang, Xiaoyan Fan, Yanxu Wang, Kun Zhang, Bing Li

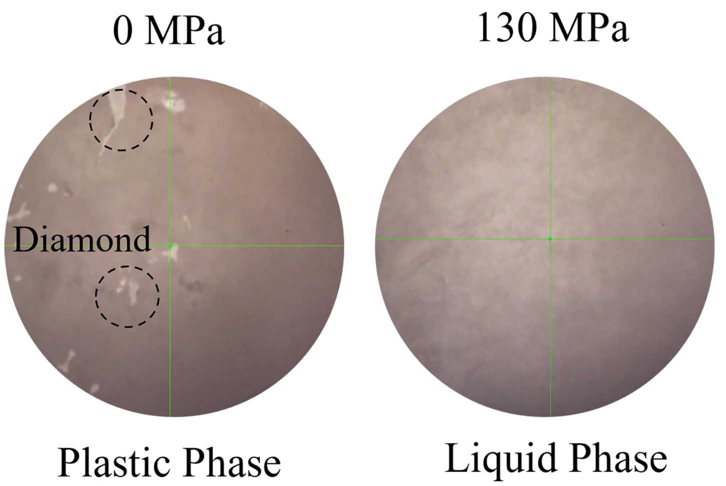

Figure S1. The optical photo for solid-liquid phase transition of 1OH corresponds to pressure-dependent Raman spectra under 0 and 130 MPa at 298 K respectively.

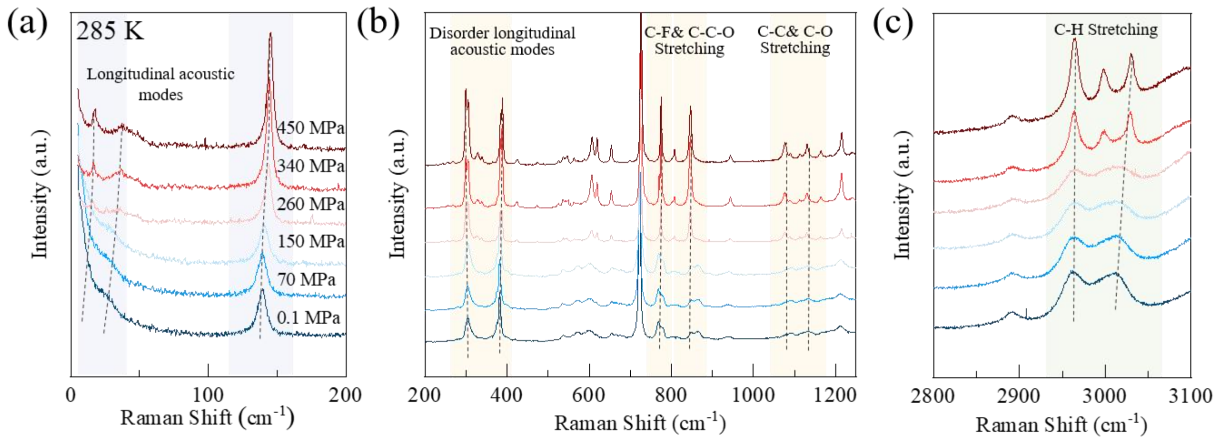

Figure S2. Pressure-dependent Raman spectra of the two phase transitions in 1OH at 285 K.

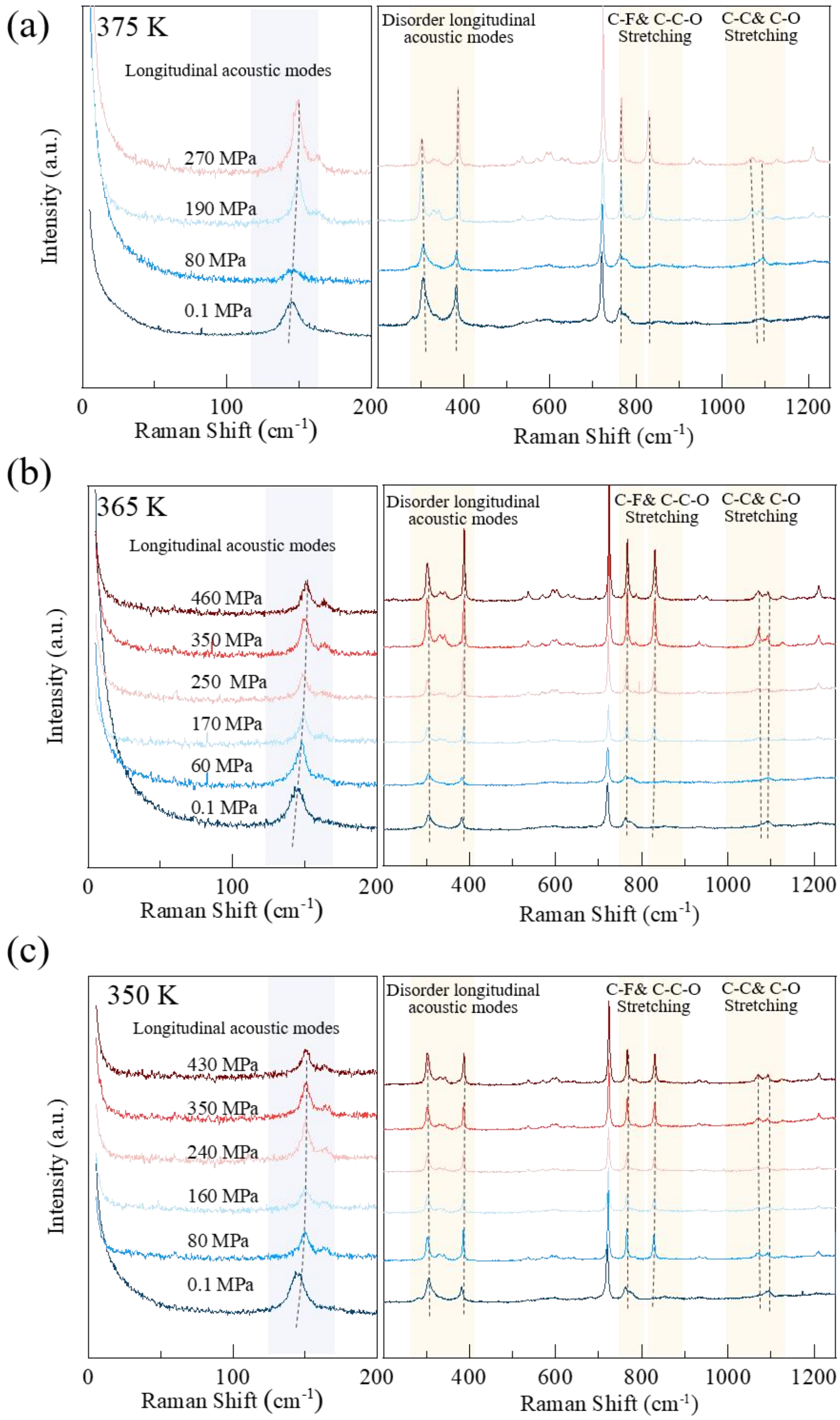

Figure S3. Pressure-dependent Raman spectra of the two phase transitions in 2OH at 350, 365 and 375 K, respectively.

Table S1. Comparison of the pressure sensitivity ($\Delta T/\Delta P$) between the current materials and other representative barocaloric (BCE) materials involving solid–liquid (S–L) and inverse transitions.

Classification	**Materials**	**$\Delta T/\Delta P$ (K/MPa)**
Solid-Liquid Phase Transition (Normal BCEs)	$C_{18}H_{38}$[1]	0.2
	$C_{16}H_{34}$[1]	0.21
	$C_{17}H_{36}$[2]	0.11
	$C_{19}H_{40}$[2]	0.11
	$C_{21}H_{44}$[2]	0.13
	$C_{12}H_{26}O$[3]	0.05
	$C_{10}H_{20}O_2$[4]	0.21
	$C_{12}H_{24}O_2$[4]	0.22
	$C_{14}H_{28}O_2$[4]	0.21
	ice[5]	0.12
Solid-Solid Phase Transition (Abnormal BCEs)	$(NH_4)_2SO_4$[6]	0.06
	$BaTiO_3$[7]	0.06
	$LaFe_{11.33}Co_{0.47}Si_{1.2}$[8]	0.1
	Mn_3GaN[9]	0.07
	$MnCoGe_{0.99}Ni_{0.01}$[10]	0.08
	$(MnNiSi)_{0.62}(FeCoGe)_{0.38}$[11]	0.08
	NH_4SCN[12]	0.3
Solid-Liquid Phase Transition (Abnormal BCEs)	2OH (This work)	0.12
	1OH (This work)	0.34

Reference

1. Lin J, Tong P, Zhang K, Tao K, Lu W, Wang X, et al. Colossal and reversible barocaloric effect in liquid-solid-transition materials n-alkanes. Nat. Commun. 2022, 13 (1): 596. DOI: 10.1038/s41467-022-28229-4.

2. Zhang Z, Li F, Xiong T, Zhang Z, Li B, Tong P, et al. Colossal Barocaloric Effects at Triple-Phase Points. Energy Environ. Mater. 2025, 8 (5). DOI: 10.1002/eem2.70021.

3. Zhang Z, Xiong T, Zhang Z, Li B, Tong P, Shen J, et al. Colossal Barocaloric Effect near Ambient Temperature in 1-Dodecanol under a Low Pressure. The Journal of Physical Chemistry Letters 2024, 15 (28): 7141-7146. DOI: 10.1021/acs.jpclett.4c01369.

4. Xiong T, Lin J, Zhou T, Shi G, Ye T, Pan X, et al. Colossal barocaloric effect of phase-change fatty acids. Appl. Phys. Lett. 2024, 125 (6). DOI: 10.1063/5.0217663.

5. Xiong T, Jiang R, Lin J, Zhou T, Shi G, Liu K, et al. Colossal barocaloric effect of water-ice phase transition. Journal of Materials Science & Technology 2026, 259: 44-51. DOI: 10.1016/j.jmst.2025.08.069.

6. Lloveras P, Stern-Taulats E, Barrio M, Tamarit J, Crossley S, Li W, et al. Giant barocaloric effects at low pressure in ferrielectric ammonium sulphate. Nat. Commun. 2015, 6 (33): 8801. DOI: 10.1038/ncomms9801.

7. Stern-Taulats E, Lloveras P, Barrio M, Defay E, Egilmez M, Planes A, et al. Inverse barocaloric effects in ferroelectric $BaTiO_3$ ceramics. APL Mater. 2016, 4 (9). DOI: 10.1063/1.4961598.

8. Mañosa L, González-Alonso D, Planes A, Barrio M, Tamarit J, Titov I S, et al. Inverse barocaloric effect in the giant magnetocaloric La–Fe–Si–Co compound. Nat. Commun. 2011, 2 (1). DOI: 10.1038/ncomms1606.

9. Matsunami D, Fujita A, Takenaka K.Kano M Giant barocaloric effect enhanced by the frustration of the antiferromagnetic phase in Mn_3GaN. Nat. Mater 2015, 14 (1): 73-8. DOI: 10.1038/nmat4117.

10. Wu R, Bao L, Hu F, Wu H, Huang Q, Wang J, et al. Giant barocaloric effect in hexagonal Ni2In-type Mn-Co-Ge-In compounds around room temperature. Sci Rep 2015, 5: 18027. DOI: 10.1038/srep18027.

11. Samanta T, Lloveras P, Us Saleheen A, Lepkowski D, Kramer E, Dubenko I, et al. Barocaloric and magnetocaloric effects in $(MnNiSi)_{1-x}(FeCoGe)_x$. Appl. Phys. Lett. 2018, 112 (2). DOI: 10.1063/1.5011743.

12. Zhang Z, Li K, Lin S, Song R, Yu D, Wang Y, et al. Thermal batteries based on inverse barocaloric effects. Sci. Adv. 2023, 9 (7): eadd0374. DOI: 10.1126/sciadv.add0374.